Fusarium verticillioides peroxins associated with peroxisomal docking/translocation module serve important roles in fumonisin biosynthesis and virulence

Wenying Yu[1,2], Mei Lin[1], Minghui Peng[2], Huijuan Yan[3], Jie Zhou[1,2], Guodong Lu[2], Won Bo Shim[3*] and Zonghua Wang[2*]

1 Fujian Province Key Laboratory of Pathogenic Fungi and Mycotoxins, College of Life Sciences, Fujian Agriculture and Forestry University, Fuzhou 350002, China

2 Fujian University Key Laboratory for Functional Genomics of Plant Fungal Pathogens, College of Plant Protection, Fujian Agriculture and Forestry University, Fuzhou 350002, China

3 Department of Plant Pathology and Microbiology, Texas A&M University, College Station, TX 77843-2132, USA

Co-corresponding authors

Won Bo Shim; TEL: +1 979 458 2190, Email: wbshim@tamu.edu

Zonghua Wang; Tel: +86 591 83789202, Email: wangzh@fafu.edu.cn

Abstract

Peroxisomes are ubiquitous organelles in eukaryotic cells that fulfill a variety of important metabolic functions. In this study, we investigated the role of Docking/Translocation Module (DTM) peroxins, mainly FvPex8, FvPex13, FvPex14, and FvPex33, in *Fusarium verticillioides* virulence and fumonisin B1 (FB1) biosynthesis. Protein interaction experiments suggested that FvPex13 serves as the core subunit of *F. verticillioides* DTM. When we generated gene deletion mutants (ΔFvpex8, ΔFvpex13, ΔFvpex14, ΔFvpex33, ΔFvpex33/14) and examined whether the expression of other peroxin genes were affected in the DTM mutants, ΔFvpex8 strain showed most drastic changes to *PEX* gene expression profiles. When we tested other physiological changes in these mutants, we observed disparity in carbon source utilization, especially sucrose and butyrate, as well as unsaturated fatty acids oleic acid and linoleic acid. Deletion mutants exhibited defect in cell wall integrity when stress agents were applied. The mutants also showed higher levels of lipid droplet accumulation when compared to WT, particularly under nutrient starvation. Notably, ΔFvpex8 mutant showed significant FB1 reduction and altered expression of *FUM1* (polyketide synthase) and *FUM19* (ABC transporter) genes. However, FvPex13 was primarily responsible for virulence when tested on maize stalks, while ΔFvpex33/14 double mutant also showed virulence defect. In summary, our study suggests that FvPex13 is the core component of *F. verticillioides* DTM, regulating peroxisome membrane biogenesis as well as PTS1- and PTS2-mediated transmembrane cargo transportation. However, FvPex8 is predicted to serve as a key component in DTM that affects peroxisome function in β-oxidation and FB1 biosynthesis in *F. verticillioides*.

Keywords*: Fusarium verticillioides*, stalk rot, Docking/Translocation, FvPex8, fumonisin B1

47 **Introduction**

48

49 Peroxisomes are a family of membrane-bound microbodies found in all major eukaryotes,
50 with specific metabolic properties showing substantial differences among various species and
51 tissue types (Alberts *et al.*, 2002, Cooper, 2000). These cellular organelles, including peroxisomes,
52 glyoxysomes in plants and fungi, glycosomes in trypanosomes, and Woronin bodies in filamentous
53 fungi, are involved in a variety of important cellular functions, including fatty acid metabolism,
54 reactive oxygen species detoxification, and secondary metabolite biosynthesis (Saikia & Scott,
55 2009, Imazaki *et al.*, 2010, Maggio-Hall *et al.*, 2005, Reverberi *et al.*, 2012, Chen *et al.*, 2018).
56 Dysfunctional peroxisomes have been shown to result in severe and lethal disorders in humans
57 and mammals (Cho *et al.*, 2018, Dixit *et al.*, 2010, Thoms *et al.*, 2009, You *et al.*, 2015). Plant
58 glyoxysomes play essential roles in glyoxylate cycle, embryonic development, and gametophytic
59 function (Hu *et al.*, 2012, Boisson-Dernier *et al.*, 2008). Glycosomes in Trypanosomes perform
60 important glycolytic reactions (Bauer & Morris, 2017). In filamentous fungi, a specific type of
61 peroxisome known as Woronin bodies are associated with septal pore maintenance and cellular
62 integrity (Jedd & Chua, 2000). Recent studies also suggest that peroxisomes play important roles
63 in development, secondary metabolism, and virulence (Kimura *et al.*, 2001, Wang *et al.*, 2013,
64 Soundararajan *et al.*, 2004), but underlying genetic mechanisms associated with these fungal-
65 specific functions still warrant further investigation.

66 *Fusarium verticillioides* is a major pathogen of maize, particularly due to ear rot disease
67 and mycotoxin contamination worldwide (Marin *et al.*, 2013, Wu *et al.*, 2014, Woloshuk & Shim,
68 2013). It is also known as the pathogen responsible for pokkah boeng in sugarcane, and
69 approximately 90% of this disease in China is attributed to *F. verticillioides* (Zhang *et al.*, 2015,

70 Hilton *et al.*, 2017, Lin *et al.*, 2014). Interestingly, Zhang et al (Zhang *et al.*, 2018b) recently
71 discovered a key peroxisomal matrix protein (FVEG_11334, which is designated as FvPex33 in
72 this study) and a Woronin body associated protein (FvHex1) interacting with Fsr1, a striatin
73 homolog that regulates virulence in *F. verticillioides*. However, gene mutagenesis experiment
74 revealed that FvPex33 and FvHex1 do not directly influence *F. verticillioides* virulence when
75 tested on maize seedlings. This outcome, along with earlier published studies on the role of
76 peroxins in fungal virulence and secondary metabolism (Fujihara *et al.*, 2010, Min *et al.*, 2012, Li
77 *et al.*, 2017) suggested that other peroxisomal matrix proteins may play important roles in *F.*
78 *verticillioides* virulence and mycotoxin biosynthesis.

79 Biogenesis of peroxisomes is dynamically regulated in response to environmental and
80 developmental cues (Lazarow, 2003, Heiland & Erdmann, 2005). Metabolic tasks and enzyme
81 content are adjusted according to taxa-specific cellular needs through generation and degradation
82 (Pieuchot & Jedd, 2012, Nuttall *et al.*, 2011). There are two primary pathways for peroxisome
83 formation; *de novo* biogenesis and mature peroxisomes fission. The *de novo* synthesis of
84 peroxisomes has two steps; formation of the peroxisomal membrane and subsequent sorting of
85 peroxisomal matrix proteins to the organelle (Opalinski *et al.*, 2011). The peroxisomal importomer
86 model helps to explain how newly synthesized matrix proteins bind to the cytosolic receptor at the
87 peroxisome membrane and form a highly dynamic pore to transfer matrix proteins to peroxisome
88 lumen (Meinecke *et al.*, 2010). These transient cargo-docking-translocation complexes are formed
89 by variable combination of peroxin (Pex) proteins (Table S1). Briefly, the key docking complex
90 core consists of the SH3-domain protein Pex13 and the PXXP-motif protein Pex14, but also
91 harbors additional species-specific factors, e.g. Pex17 in lower eukaryotic cells, Pex33 (also
92 known as Pex14/17) in filamentous fungi, and Pex13.2 in *Trypanosoma brucei* (Verplaetse *et al.*,

93 2012). A recent study also characterized Pex17/Pex14/Dyn2p complex in yeast (Chan *et al.*, 2016).
94 Physical association among docking peroxins varies in different organisms, and recent reviews
95 extensively explain how various matrix proteins with type 1 and type 2 peroxisomal targeting
96 signal (PTS1 and PTS2) are recognized by the specific docking complex and associate with the
97 peroxisomal membrane (Nuttall *et al.*, 2011, Pieuchot & Jedd, 2012).

98 PTS1 and PTS2 peroxisomal matrix proteins are recognized by specific receptors Pex5 and
99 Pex7, respectively, and recruited to the peroxisome docking complex (Meinecke *et al.*, 2010,
100 Heiland & Erdmann, 2005). In addition to these core Peroxins, other Pex proteins are dynamically
101 involved in translocating matrix proteins across the peroxisome membrane (Platta *et al.*, 2013). In
102 particular, Pex8 is known to be associated with docking/translocation module (DTM) but is only
103 present in yeasts and filamentous fungi (Agne *et al.*, 2003). It has been suggested that Pex8 can
104 serve as a importomer-bridging protein to hold the docking complex and the export machinery
105 complex together to facilitate dynamic and transient translocation (Rayapuram & Subramani, 2006,
106 Platta *et al.*, 2013, Meinecke *et al.*, 2010), but the detailed function is largely unknown. In this
107 study, our aim was to characterize putative *F. verticillioides* peroxins, particularly those predicted
108 to be involved in DTM. We paid close attention to two core components of the docking complex,
109 Pex13 and Pex14, but also expanded our study into additional matrix proteins, namely Pex8, that
110 have not been well studied in plant pathogenic fungi. Subsequently, we studied the physical
111 interactions and the functional role of each component in *F. verticillioides* through targeted gene
112 deletion experiments. Through a series of fungal metabolism, physiology and virulence assays, we
113 concluded that Pex8, along with Pex13, plays a critical role in the generation of docking complex
114 in peroxisomes and for peroxisome function in *F. verticillioides* virulence and mycotoxin
115 biosynthesis.

116

117 **Results**

118

119 **Protein-protein interactions between *F. verticillioides* DTM components and other key**
120 **peroxins**

121 Peroxins Pex13 and Pex14 are recognized as key peroxisomal membrane docking complex
122 proteins in eukaryotes, which are required for protein import into peroxisomes. In addition, Pex33
123 has been identified as a new component of the docking complex in *Neurospora crassa* (Managadze
124 *et al.*, 2010), and Pex8 is known to be associated with DTM in yeasts and filamentous fungi (Agne
125 *et al.*, 2003). Using these proteins as query, we screened for putative DTM components, *i.e.* Pex13,
126 Pex14, Pex33, and Pex8, in *F. verticillioides* using the BLASTP algorithm. Additional details for
127 these key Pex proteins, e.g. sequence similarities and putative functional motifs, are provided in
128 Supplementary Information (Table S1 and Fig. S1A). Notably, further comparison of FvPex33
129 against Pex14- and Pex17-like proteins in *S. cerevisiae*, *F. graminearum*, *F. verticillioides* strongly
130 suggested that FvPex33 is distinct from Pex14 and Pex17 and is a unique component of DTM in
131 *F. verticillioides* (Fig. S1B).

132 Based on TMPRED, FvPex8, FvPex13, FvPex14, and FvPex33 are predicted to have
133 transmembrane helices and likely belong to peroxisomes membrane proteins (Fig. S1C). To study
134 the cellular localization of these proteins in *F. verticillioides*, we first chose the biogenesis protein
135 Pex14 as the peroxisomal marker and prepared Pex14-mCherry construct (Grant *et al.*, 2013). We
136 studied transformants containing GFP-fused Pex8, Pex13, or Pex33 protein along with Pex14-
137 mCherry for overlapping red and green fluorescence signals (Fig. 1A), and the images revealed
138 Pex14 co-localizing with Pex13 and Pex33 while only showing partial overlap with Pex8. We

139 subsequently tested physical interactions between these DTM components and other Peroxins by
140 yeast two-hybrid assays (Fig. S2). FvPex13 showed positive interaction with all five peroxins
141 tested, whereas FvPex14 showed interaction with FvPex5, FvPex7, FvPex33 and FvPex14 itself.
142 FvPex8 showed interactions with FvPex7, but not with FvPex14 and FvPex33 (Fig. S2). We also
143 learned that FvPex8 BD and FvPex5 BD can self-activate (data not shown), and therefore we did
144 not test the interaction between FvPex8 and FvPex5.

145 To further verify interactions between key DTM subunits and peroxins, we transiently co-
146 expressed following six pairs of proteins, *i.e.* FvPex13-GFP/FvPex14-mCherry, FvPex13-
147 GFP/FvPex8-mCherry, Pex33-GFP/Pex14-mCherry, and Pex8-GFP/Pex14-mCherry, into *F.*
148 *verticillioides* for coimmunoprecipitation (Co-IP) experiments. Results showed that FvPex13-GFP
149 successfully associated with the beads and that FvPex14 was eluted in samples that co-expressed
150 FvPex13-GFP and FvPex14-mCherry, indicating Pex13 and Pex14 binding *in vivo* (Fig. 1B).
151 Similarly, FvPex13 successfully associated with FvPex8 (Fig. 1C). FvPex33 successfully
152 associated with FvPex14 (Fig. 1D), but FvPex8 did not coprecipitate with FvPex14 (Fig. 1E).
153 FvPex13 showed direct interaction with key DTM proteins, and based on these outcomes, we
154 concluded that FvPex13 serves as the core subunit in *F. verticillioides* DTM.

155

156 **Phenotypic characterization of DTM peroxin gene deletion mutants**

157 To study the function of key DTM peroxins in *F. verticillioides*, we generated ΔFvpex8,
158 ΔFvpex13, ΔFvpex14, and ΔFvpex33 through targeted gene replacement with the hygromycin-
159 resistance marker in *F. verticillioides* 7600 wild-type strain as described previously (Zhang *et al.*,
160 2018b). We also generated ΔFvPex33/14 double mutant by replacing *FvPEX14* gene with the
161 geneticin-resistance marker in ΔFvpex33 protoplast. Subsequently, we also generated

162 complementation strains ΔFvpex8-C, ΔFvpex13-C, ΔFvpex14-C, and ΔFvpex33-C by
163 transforming the corresponding mutant with a construct harboring the gene (with its native
164 promoter and terminator) fused with GFP and the geneticin resistance marker. Homologous
165 recombination was confirmed by polymerase chain reaction (PCR) the gene and quantitative PCR
166 (qPCR) the expression of the gene in corresponding complementation strains (Data not shown).
167 We first examined whether expression of other peroxin genes were affected in the DTM
168 mutants (Fig. 2A). These included four DTM genes (*FvPEX8*, *FvPEX13*, *FvPEX14* and *FvPEX33*),
169 two PTS receptor genes (*FvPEX5* and *FvPEX7*), and a membrane protein receptor gene
170 (*FvPEX19*). *FvPEX8* exhibited no detectable change when tested in three other DTM mutants.
171 *FvPEX13* showed decreased expression while *FvPEX14* and *FvPEX33* showed drastically
172 increased expression in ΔFvpex8 mutant. *FvPEX5* and *FvPEX7* genes showed elevated
173 transcription levels in ΔFvpex8 mutant while showing decreased transcription in ΔFvpex33/14
174 mutant when compared with the wild type. Meanwhile, *FvPEX19* was suppressed in ΔFvpex8,
175 ΔFvpex33, ΔFvpex33/14 mutants. When comparing DTM mutants, deletion of *FvPEX8* led to
176 most noteworthy changes in peroxin gene expression, particularly dramatic overexpression of PTS
177 receptor genes (*FvPEX5* and *FvPEX7*) as well as two DTM genes (*FvPEX14* and *FvPEX33*) led
178 us to hypothesize that FvPex8 plays an important role in maintaining peroxisomal membrane
179 assembly and cargo transport machinery. It is also notable that ΔFvpex33/14 double mutant, but
180 not ΔFvpex14 or ΔFvpex33 single mutant, exhibited strong negative impact on expression of
181 *FvPEX5, FvPEX7, FvPEX14* and *FvPEX33.*
182
183 **Vegetative growth and conidiation are differentially affected by carbon sources in DTM**
184 **peroxin mutants**

185 The colony morphology of the DTM mutants was similar to that of the wild-type progenitor
186 when compared on MM (Fig. 2B), suggesting that these genes are not essential for vegetative
187 growth. However, we observed a drastic reduction in conidiation in ΔFvpex13 and ΔFvpex33/14
188 mutants on CMII agar medium (Fig. S3C). We also learned that vegetative growth and aerial
189 mycelia production in ΔFvpex8 and ΔFvpex33/14 were significantly hindered on agar media with
190 butyrate and sucrose as the primary carbon source (Fig. 2B and 2C). When cultured on media with
191 acetate, all mutants were indistinguishable when compared to the wild type (Fig. 2B and 2C).
192 Restricted growth was also observed when mutants were grown on media with unsaturated long-
193 chain fatty acids. ΔFvpex8 and ΔFvpex33/14 mutants showed hindered vegetative growth on a
194 medium with palmitic acid and oleic acid (Fig. 2B and 2C). Interestingly, aerial mycelium was
195 completely absent in ΔFvpex8 mutant on media with palmitic acid. The growth was not severly
196 hindered in ΔFvpex8 and ΔFvpex13 mutants grown on medium with oleic acid, but aerial mycelia
197 production was not as vigorous as the wild type. *F. verticillioides* DTM mutants showed difficulty
198 growing on long fatty acids palmitic acid raising the hypothesis whether these peroxins play a role
199 in peroxisomal β-oxidation function. When investigating *F. verticillioides* PTS proteins *in silico*,
200 we also learned that palmitoyl-CoA hydrolase (FVEG_02271, designated FvAct) contains PTS1
201 and serine palmitoyl transferase (FVEG_12143, designated FvPat) contains PTS2. We can
202 postulate that FvPex8 indirectly impacts hydrolysis of palmitoyl-CoA, which is an acyl-CoA
203 thioester that plays a role in biosynthesis of sphingolipids and in transport of fatty acyl-CoA
204 molecules into the mitochondria for β-oxidation (Brady *et al.*, 1969).
205
206 **Redox homeostasis, cell wall integrity, and lipid degradation in DTM mutants**

207 Peroxisomes serve as one of the primary sources of endogenous and exogenous ROS
208 production. Accumulation of ROS and disruption of redox homeostasis can lead to lower cell
209 survival (Min *et al.*, 2012). When stained with CM-H2DCFDA, mutant hyphae showed green
210 fluorescent granules indicative of high ROS accumulation, especially in ΔFvpex8, ΔFvpex13 and
211 ΔFvpex33/14 mutants (Fig. 3A and 3B). The colonies were stained with 3,3'-diaminobenzidine
212 (DAB) and nitro blue tetrazolium (NBT) for H_2O_2 and O^2- detection, respectively. Yellow and blue
213 colonies were observed in ΔFvpex8, ΔFvpex13, and ΔFvpex33/14 mutants with DAB and NBT
214 staining, respectively (Fig. 3C). Peroxin mutants are likely to display cell wall integrity defects
215 due to their inability to import enzymes of the glyoxylate cycle into peroxisomes (Bhambra et al.
216 2006). Almost all mutants exhibited sensitivity to calcofluor while except for ΔFvpex8 mutant
217 (Fig. 4). Mutants showed much higher sensitivity in general to sodium dodecyl sulfate (SDS) when
218 compared to the wild type (Fig. 4). Growth inhibition rate in peroxin mutants was significantly
219 higher than that of wild type, suggesting DTM peroxins are important for maintaining *F.*
220 *verticillioides* cell wall integrity. We also observed growth inhibition in DTM mutants on medium
221 amended with H_2O_2 when compared to the WT (Fig. 4), which suggested that ability to respond to
222 reactive oxygen species and maintain redox homeostasis was disturbed in these peroxin mutants.
223 We also studied lipid droplet degradation and turnover defects in DTM mutants. The mutants
224 accumulated higher levels of lipid droplets compared to WT, particularly when shifted to nutrient
225 starvation (Fig. S4).
226

227 **DTM peroxin FvPex8 function is necessary for FB1 production in *F. verticillioides***

228 *F. verticillioides* is one of the key fungal pathogens responsible for fumonisin
229 contamination of maize worldwide. To assess fumonisin B1 (FB1) accumulation, we

230 independently inoculated B73 maize kernels with spore suspensions of WT, ΔFvpex8, ΔFvpex13,
231 ΔFvpex14, ΔFvpex33, and ΔFvpex33/14 strains. After 10 days of incubation, fungal mass in
232 samples was assessed by qPCR quantification of β-tubulin gene *TUB2* DNA. Fungal mass in
233 ΔFvpex8, ΔFvpex13 and ΔFvpex33/14 mutants was approximately half of those observed in WT,
234 ΔFvpex14, and ΔFvpex33 (Data not shown). When FB1 levels were normalized to fungal mass in
235 each sample, all mutants showed reduction in FB1 production, ranging from 50% to 94%, with
236 ΔFvpex8 showing the most drastic reduction (Fig. 5A).

237 To further understand how FvPex8 mutation resulted in such drastic reduction in FB1
238 biosynthesis, we analyzed transcriptional expression of four key *FUM* genes: polyketide synthase
239 *FUM1*, aminotransferase *FUM8*, transporter *FUM19*, and transcription factor *FUM21* (Bojja *et al.*,
240 2004, Desjardins & Proctor, 2007, Brown *et al.*, 2007). The expression levels of these genes were
241 assessed by qPCR in WT and ΔFvpex8 strains after a 10-day incubation on corn kernels (Fig. 5B).
242 When compared to the WT, the expression of these four genes were significantly suppressed in
243 ΔFvpex8, particularly *FUM1* and *FUM19* showing drastically lower expression levels (Fig. 5B).
244 These outcomes suggest that FvPex8 function is necessary for proper expression of FUM genes in
245 *F. verticillioides*, not only those involved in biosynthesis but also fumonisin transport mechanism
246 mediated by *FUM19*.

247

248 **DTM peroxin FvPex13 plays key roles in *F. verticillioides* virulence**

249 To test whether these DTM Peroxins are associated with virulence, we inoculated B73
250 maize stalk internodes with spore suspension of the wild-type, ΔFvpex8, ΔFvpex13, ΔFvpex14,
251 ΔFvpex33, and ΔFvpex33/14 strains. When stalks were split open longitudinally after a 10-day
252 incubation, ΔFvpex13 and ΔFvpex33/14 mutants showed drastically reduced rot when compared

253 with the wild-type progenitor and other mutants (Fig. 6). We further tested virulence on sugar cane
254 (cultivar Badila), and outcomes were quite similar to those observed in maize stalk rot assays with
255 ΔFvpex13 showing significantly decreased levels of rot (Fig. S5). It is notable while ΔFvpex14
256 and ΔFvpex33 single mutations did not impact stalk rot, the double mutant ΔFvpex33/14 showed
257 a significant reduction in virulence when tested on maize and sugarcane stalks (Fig. 6 and S5).
258 Also, ΔFvPex8 mutation did not have any negative impact on *F. verticillioides* virulence.
259 FvPex13-complemented strain showed wild type-level stalk rot symptoms, suggesting that
260 FvPex13 plays a critical role in *F. verticillioides* virulence on maize and sugarcane.
261

262 **Deletion of Pex13 impacts cellular localization of DTM peroxins in *F. verticillioides***

263 A mutation in Pex13 has been linked to PTS1 import defects in yeast, peroxisome
264 abnormalities and appressorium defects in *Colletotrichum orbiculare* (Erdmann & Blobel, 1996,
265 Fujihara *et al.*, 2010). To monitor PTS matrix protein import in *F. verticillioides*, we used confocal
266 microscopy to follow GFP derivatives targeted to the peroxisome. We fused GFP to carnitine O-
267 acetyl transferase gene *FvCAT* containing C-terminal PTS1 sequence (Zolman & Bartel, 2004) or
268 peroxisomal 3-oxoacyl-CoA thiolase gene *FvFOX3* containing *N*-terminal PTS2 sequence
269 (Einerhand *et al.*, 1995) obtaining fusion protein GFP-PTS1 and PTS2-GFP, respectively. We also
270 tested physical interactions between these two PTS proteins and PTS receptor proteins by yeast
271 two-hybrid assays; FvPex5 showed positive results with FvCAT and FvPex7 showed positive
272 results with FvFOX3 (Fig. S2). GFP-PTS1 showed a diffused fluorescence distributed throughout
273 the cytoplasm while PTS2-GFP was largely in cytoplasm of 2-days-old ΔFvpex13 hyphae (Fig.
274 7A). Pex14-mCherry is shown as the peroxisomal marker. These results led us to hypothesize that
275 FvPex13 plays a role in peroxisomal protein targeting via its interaction with FvPex5 and FvPex7.

276 We learned that PTS1 receptor FvPex5 predominantly localizes to the cytoplasm, very similar to
277 FvCat, whereas PTS2 receptor FvPex7 and mPTS receptor FvPex19 are mostly found in cytoplasm
278 in ΔFvpex13 mutant (Fig. 7B). These results suggested that FvPex13 function is not only required
279 to maintain localization but also affect the steady-state size and number levels of these docking
280 peroxins affecting peroxisomes.
281
282 **Discussion**
283
284 The key aim of this study was to gain a deeper understanding of how peroxisomal
285 docking/translocation module (DTM) complex impacts peroxin import, the integrity and
286 functionality of peroxisomes, and ultimately fumonisin biosynthesis and virulence in maize
287 pathogen *F. verticillioides*. Interaction between four DTM peroxins, *i.e*. FvPex13, FvPex14,
288 FvPex33 and FvPex8, were demonstrated through yeast two-hybrid and Co-IP assays.
289 Interestingly, FvPex8 exhibited no direct interaction with FvPex14 and FvPex33. We also
290 confirmed that FvPex14-mCherry colocalizes with FvPex13-GFP, FvPex8-GFP, and FvPex33-
291 GFP in mycelia, suggesting that these proteins form a complex in *F. verticillioides*. In ΔFvpex13,
292 we found that FvPex5 (PTS1 receptor), and FvCat (PTS1), FvPex7 (PTS2 receptor), FvFox3
293 (PTS2), FvPex8, FvPex19 were predominantly translocated to cytoplasm, while FvPex14 and
294 FvPex33 were still remaining in peroxisomes. FvPex13 played a more predominant role in PTS1
295 than PTS2 though FvPex13 interactive with both PTS receptor. In *S. cerevisiae*, Pex14
296 preferentially binding to cargo-loaded Pex5 receptor are responsible for pore formation, while
297 Pex13 can Co-IP Pex5 but not a Pex5–PTS1 complex, higher affinity to the free receptor and is
298 involved in coupling of translocation to receptor recycling (Schell-Steven *et al.*, 2005). It was

299 suggested that Pex13 served as an initial binding site for the PTS2 pre-import complex, whereas
300 Pex14 assembled with Pex18 in high-molecular-weight complexes after or during dissociation of
301 the PTS2 receptor (Grunau *et al.*, 2009, Meinecke *et al.*, 2010). Based on literature and our
302 experimental data, we envisaged a schematic model of *F. verticillioides* peroxisomal DTM
303 complex shown in Fig. 8. We suggest that FvPex14 and Fvpex33 prefer the initial recognition of
304 the PTS1 cargo-loaded receptor and PTS2 cargo-loaded receptor respectively, while FvPex13 and
305 FvPex8 prefer to unload cargo-loaded from the receptor.

306 Recent studies provide numerous examples how key DTM proteins Pex13 and Pex14 are
307 important not only for peroxisome biogenesis but also for hosts of other cellular and physiological
308 functions in filamentous fungi. Absence of the docking peroxin Pex13 in *Podospora anserine*
309 obstructed sexual development prior to meiosis (Suaste-Olmos *et al.*, 2018) *Colletotrichum*
310 *orbiculare* Pex13 is required for appressorium-mediated plant infection, namely for melanin
311 biosynthesis and turgor generation (Fujihara *et al.*, 2010, Chen *et al.*, 2018). Chen and colleagues
312 (Chen *et al.*, 2018) showed that Pex13 also plays an important role in *Fusarium graminearum*
313 pathogenesis and mycotoxin biosynthesis. We found very similar outcomes in our study, where *F.*
314 *verticillioides* Pex13 mediated plant infection and severe peroxisomal defects. Pex14, in addition
315 to its key function as a docking protein, plays a main role in formation of two separate import
316 pores, facilitating the PTS1- and PTS2-dependent protein import into the peroxisomal matrix
317 (Montilla-Martinez *et al.*, 2015, Meinecke *et al.*, 2010). Pex14 has a unique dual function in
318 peroxisome formation and in pexophagy in *Pichia pastoris* and *F. graminearum* (Bellu *et al.*, 2001,
319 Farre *et al.*, 2008, Deng *et al.*, 2013, Lee *et al.*, 2017, Chen *et al.*, 2018). Pex14 serves an important
320 role in Woronin bodies formation in *Neurospora crassa* and host infection in *Fusarium*
321 *graminearum* (Managadze *et al.*, 2007, Chen *et al.*, 2018). In addition to Pex13 and Pex14, another

322 important component of DTM complex in filamentous fungi is Pex33, a chimeric protein
323 consisting of an N-terminal Pex14-like domain and a C-terminal Pex17-like domain . Pex33 has
324 been associated with glyoxysome biogenesis, sexual and asexual development, virulence and
325 secondary metabolism (Peraza-Reyes *et al.*, 2011, Li *et al.*, 2017, Chen *et al.*, 2018, Opalinski *et*
326 *al.*, 2010, Managadze *et al.*, 2010). In our study, we found *F. verticillioides* Pex14 and Pex33
327 collaborate to mediate plant infection and partial peroxisomal defects.

328 While these key Pex proteins have been extensively investigated in filamentous fungi and
329 other eukaryotes, the role of Pex8 in peroxisomal import machinery and its impact on other
330 physiological roles in pathogenic fungi are still unclear. Pex8, originally discovered as Per1 protein
331 in yeast *Hansenula polymorpha* (syn. *Pichia angusta*), is an intraperoxisomal peroxin that has a
332 PTS1 at the C- terminus and an unusual PTS2 in the mid-protein region (Agne *et al.*, 2003,
333 Waterham *et al.*, 1994). Pex8 is currently the only recognized intraperoxisomal peroxin, while
334 majority of peroxins are either peroxisomal membrane-bound or in the cytosol (Ma *et al.*, 2009,
335 Pieuchot & Jedd, 2012, Girzalsky *et al.*, 2010). Pex8 is targeted to peroxisomes by cytosolic
336 receptors Pex5 (PTS1) or Pex7 (PTS2), and the membrane translocation is primarily mediated
337 through docking complex Pex14 (Agne *et al.*, 2003, Ma *et al.*, 2009). Once positioned in the
338 peroxisomal matrix, Pex8 becomes an important component of importomer complex, anchoring
339 key receptors as well as other membrane-bound peroxins, and serves an important function in both
340 PTS1- and PTS2-dependent protein translocation into peroxisome (Agne *et al.*, 2003, Rehling *et*
341 *al.*, 2000). Therefore, it is important to acknowledge that composition and organization of the
342 importomer and docking complex can vary in eukaryotes, not only in species-dependent manner
343 but also in a cargo-dependent manner (Gabaldon, 2010, Heiland & Erdmann, 2005, Lazarow,
344 2003).

345 In our study, we learned that Pex8 plays a crucial role in *F. verticillioides* secondary
346 metabolism but is dispensable for plant pathogenesis. Involvement of peroxisomes in fungal
347 secondary metabolite biosynthesis has been well documented, including in penicillin, AK toxin,
348 paxilline, and deoxynivalenol (DON) (Herr & Fischer, 2014, Saikia & Scott, 2009, Imazaki *et al.*,
349 2010, Martin *et al.*, 2012, Chen *et al.*, 2018). However, it is still unclear how FvPex8 impacts FB1
350 biosynthetic pathway or regulation. We learned that the expression of *FUM1* and *FUM19* is
351 decreased drastically in ΔFvpex8 mutant, but it is highly unlikely FvPex8 directly regulates genes
352 in the *FUM* cluster. However, it is possible that Pex8, which contains both peroxisomal targeting
353 signals PTS1 and PTS2, functions as an organizer of the peroxisomal protein import machinery.
354 In *S. cerevisiae*, Pex8 is located at the inner surface of the peroxisomal membrane and is essential
355 for the assembly of the importomer (Deckers *et al.*, 2010). Acetyl-CoA, one of the key buildings
356 block for the synthesis of polyketides, can be produced via various catabolic pathways, including
357 peroxisomal β-oxidation of fatty acids (Maggio-Hall *et al.*, 2005). Based on current DTM models,
358 inner membrane FvPex8 function may impact both import receptors Pex5 (PTS1 cargo shuttle)
359 and Pex7 (PTS2 cargo shuttle) and disrupt import/export of acetyl-CoA necessary for secondary
360 metabolism in *F. verticillioides*. While higher expression levels of *FvPEX5* and *FvPEX7* were
361 observed in ΔFvpex8 mutant, further study is needed to test this hypothesis.

362 One unexpected outcome in our study was ΔFvpex8 showing no particular defect in virulence.
363 Key peroxisome biogenesis genes are required plant infection and pathogenesis in *Colletotrichum*
364 *lagenarium, C. orbiculare, M. grisea, A. alternata,* and *F. graminearum* (Ramos-Pamplona &
365 Naqvi, 2006, Wang *et al.*, 2007, Imazaki *et al.*, 2010, Fujihara *et al.*, 2010, Goh *et al.*, 2011, Min
366 *et al.*, 2012). For instance, CoPex13 is required for appressorium melanization and turgor
367 generation, which are essential for appressorium penetration ability in *C. orbiculare* (Fujihara *et*

368 *al.*, 2010). MoPex33 is required for import of peroxisomal matrix proteins and full virulence in *M.*
369 *oryzae* (Li *et al.*, 2017). A recent publication described how Pex13, Pex14 and Pex33 are critical
370 against host stress agents and pexophagy, ultimately impacting fungal virulence in *F.*
371 *gramminearum* (Chen *et al.*, 2018). Along with these key DTM components, import receptors
372 Pex5 and Pex7 were also shown to be important for fitness and virulence in fungal pathogens (Min
373 *et al.*, 2012, Wang *et al.*, 2013, Zhang *et al.*, 2018a, Goh *et al.*, 2011). FvPex8 showed strong
374 physical interaction with FvPex13, therefore it was reasonable to hypothesize that FvPex8 also
375 plays a critical role in pathogenesis. However, this was not the case; only ΔFvpex13 was impaired
376 in virulence in *F. verticillioides* (Fig. 6). FvPex13 is known to affect efficient PTS1 and PTS2
377 imports, and this requires Pex5-Pex13 interaction *in vivo* (Pires *et al.*, 2003, Schell-Steven *et al.*,
378 2005). Loss of peroxisome function may slow pathogen growth due to inefficient utilization of
379 carbon sources from the host and the fungus itself (Fig. 2B and S4). However, we did not observe
380 similar response in host when challenged by ΔPex8 mutant suggesting that Pex8, while it forms a
381 complex with Pex13 and other DTM components, may not directly contribute to virulence in F.
382 verticillioides.

383 To summarize, we identified and characterized *F. verticillioiodes* homologs of DTM
384 components FvPex13, FvPex14, FvPex33, and FvPex8 in this study. Based on our experimental
385 outcomes and literature, we propose a schematic model of core *F. verticillioides* DTM complex
386 (Fig. 8). It is reasonable to hypothesize that these proteins are involved in the regulation of
387 peroxisomal docking complex assembly and matrix translocation and ultimately impact various
388 aspects of fungal development, secondary metabolism, and virulence. However, we clearly noticed
389 a distinct role each component plays. We propose that the DTM complex plays an important role
390 in virulence through FvPex13, likely in association with FvPex14 and FvPex33. For FB1

391 production, FvPex8 was determined as the key components, but the mechanism in which FvPex8
392 regulates FB1 biosynthesis needs further investigation.
393
394 **Material and methods**
395
396 **Fungal strains and culture media**
397 *F. verticillioides* wild-type strain 7600 and all transformants (Table S2) were cultured on complete
398 medium (CMII: 2% sucrose, 0.05% magnesium sulfate heptahydrate, 0.1% potassium dihydrogen
399 phosphate, 0.05% potassium chloride, 0.2% nitrate potassium acid, 0.1% hydrolyzed casein, 0.2%
400 peptone, 0.1% Wolfe's Vitamin Solution [Coolaber, China], 1.8% agar) and minimal medium
401 (MM) (Leslie & Summerell, 2006). CMII agar with 250 μg/ml hygromycin B (Roche, Germany),
402 200 μg/ml glufosinate-ammonium (Sigma, USA) or 800 μg/ml G418 (Sigma) were used for
403 screening transformants. For conidia production assay, six 0.7 cm- diameter agar blocks were
404 added to 3 ml water, vortexed and conidia were quantified by a hemocytometer. For vegetative
405 growth and stress agent sensitivity assays, the wild-type and mutant strains were grown on MM
406 supplemented with various carbon sources at the following concentrations: potassium acetate (40
407 mM), sodium butyrate (10 mM), sucrose (2%), palmitic acid (3 mM), oleic acid (3 mM) and
408 linoleic acid (3 mM) (Min *et al.*, 2012). Colony diameter was measured after 5 days of incubation.
409 Cell wall integrity was tested by growing the strains on CMII supplemented with 200mg/ml
410 Calcofluor white (CFW) or 0.01% sodium dodecyl sulfate (SDS). The tolerance of strains to
411 exogenous ROS was evaluated by measuring growth on CMII containing 0.05% H_2O_2.
412
413 **Generation of the DTM gene deletion mutants and GFP/mCherry-tagged strains**

414 Single DTM gene *F. verticillioides* mutants were generated with a split-marker approach
415 described previously (Zhang *et al.*, 2018b). All primers used in this study are listed in Table S3.
416 For double deletion of *FvPEX14* and *FvPEX33*, we replaced the *FvPEX14* with neomycin
417 phosphotransferase (*NEO*) gene in the ΔFvpex33 deletion mutant. Protoplasts were generated,
418 transformed and screened following our standard PCR and Southern blot protocols (Yan & Shim,
419 2020, Zhang *et al.*, 2018b). We constructed the fusion GFP and mCherry vectors following the
420 protocol described previously (Zhang *et al.*, 2018b, Yan & Shim, 2020). All fusion vectors
421 generated were sequenced before transformation. For construction of GFP-tagged strains, we
422 transformed corresponding fusion GFP vectors with G418 sulfate-resistant (*GEN*) gene into
423 protoplasts. For testing whether FvPex13 affected the localization of PTS pathway related genes,
424 we transformed fusion GFP vectors with *GEN* into WT and ΔFvPex13 mutant protoplasts.
425
426 **Expression analyses of peroxin genes**
427 For qRT-PCR, the wild-type and DTM mutants were inoculated in CMII medium for 3
428 days. The extraction of total RNA and the synthesis of first-strand cDNA were performed as
429 previously described (Yan & Shim, 2020). The expression of peroxins, were detected by qRT-
430 PCR using SuperReal PreMix Plus (SYBR Green) (Tiangen Biotech, China). As an endogenous
431 control, a 200-bp amplicon of *F. verticillioides* β-tubulin (*TUB2*) gene (FVEG_04081) was
432 amplified, and the relative quantification of each transcript was calculated following the standard
433 $2^{-\Delta\Delta CT}$ method (Yan & Shim, 2020). Primers used to amplify selected genes in qRT-PCR reactions
434 are listed in Table S3. All qRT-PCR assays were conducted in triplicates for each sample and the
435 experiment was repeated three times.
436

437 **ROS and lipid staining and quantification**

438 For lipid staining, 2-day-old mycelia were harvested and washed twice with water. Hypha
439 was tested by staining with Nile Red (Nguyen *et al.*, 2011). Cellular ROS accumulation in the
440 fungal hyphae was analyzed using the CM-H2DCFDA staining. Mycelia were harvested and
441 washed with PBS for 3 times. Hypha was stained with CM-H2DCFDA (5 μM) (Sigma) for 10 min
442 in the dark following GENMED reagent protocols, scanning confocal microscope with excitation
443 at 490nm (GENMED Scientifics, USA). Accumulation of ROS in mycelia was visualized with 6-
444 chloromethyl-2',7'-dichlorodihydrofluorescein diacetate (CM-H2DCFDA) staining. Endogenous
445 ROS scavenging capacity was tested by growing the strains on CMII medium 5 days, and the
446 colony were stained with 3,3'-diaminobenzidine (DAB) for H_2O_2 detection and with 2mM Nitro
447 Blue Tetrazolium (NBT) (Sigma) in 20mM phosphate buffer, pH6 for O^{2-} detection treated,
448 respectively.

449

450 **Yeast two-hybrid assay**

451 The yeast two-hybrid assay was carried out following our previous standard protocol
452 (Zhang *et al.*, 2018b). The coding sequence of each tested gene was amplified from wild-type
453 cDNA. *FvPEX13*, *FvPEX14*, *FvPEX7*, and *FvCAT* were cloned into pGBKT7 as the bait vectors.
454 Other components of the DTM *FvPEX33*, *FvPEX14*, *FvPEX8*, *FvPEX5*, *FvPEX7*, *FvPEX20*,
455 *FvFOX* cDNA was amplified and cloned into pGADT7 as the prey vectors. The pairs of plasmids
456 pGBKT7-P53 and pGADT7-T, pGBKT7-Lam and pGADT7-T were used as the positive and the
457 negative control, respectively. All primers used in this study were listed in Table S3. Further details
458 are provided in Supplementary Information.

459

460 **Virulence and FB1 assays**

461 Infection assays on maize and sugarcane stalks were conducted as previously described
462 (Zhang *et al.*, 2018b, Zhang *et al.*, 2015). Subsequently, maize and sugar cane stalks were split
463 longitudinally to assess disease severity and to quantify the extent of the rot by Image J software.
464 For FB1 assay, conidia were inoculated on surface sterilized B73 corn kernel for 10 days and
465 quantified with Fumonisin B1 ELISA Kit following manufacturer's suggested protocol (Biovision,
466 USA). FB1 concentrations were obtained by the optical density (OD value) of each well at 450 nm
467 with a microplate reader by comparing to FB1 standard curve. *F. verticillioides* biomass
468 quantification was calculated by qPCR based on the *TUB*2 standard curve, which was measured
469 at 0.01, 0.1, 1.0, 10 ng/μl concentrations (Rocha *et al.*, 2015). Sample FB1 levels were normalized
470 by calculating FB1 ppm/ *TUB*2 DNA concentration. To compare the *FUM* gene expression, RNA
471 samples were prepared from ΔFvpex8 mutant and *F. verticillioides* strains grown on corn kernel
472 for 10 days. The expression levels of *FUM1*, *FUM8*, *FUM19* and *FUM21* were normalized to
473 *TUB2* expression. The experiment was repeated three times.

474

475 **Immunoblot and immunoprecipitation analyses**

476 Strains were grown in CMII medium for 2 days before immunoblot and
477 immunoprecipitation analyses were conducted as previously described (Zheng *et al.*, 2015). For
478 total protein extraction, mycelia of FvPex13-GFP and FvPex14-mCherry were ground into a fine
479 powder in liquid nitrogen and resuspended in 30-mL extraction buffer (10 mM Tris/Cl pH 7.5, 150
480 mM NaCl, 0.5 mM EDTA, 0.5% NP40, 1 mM PMSF). The supernatants were centrifuged 15,000
481 g for 25 min at 4°C to remove cell debris. For immunoprecipitation of GFP-fusion proteins from
482 cellular extracts, equal concentration of total proteins was isolated and incubated with 20~30 μL

483 of GFP-Trap agarose beads (ChromoTek, Germany) according to manufacturer's instructions.
484 Proteins eluted from GFP-Trap agarose beads were analyzed by immunoblot detection with the
485 anti-mCherry (Clontech, USA) and anti-GFP (Sigma) antibodies.
486

487 **Author Contributions**

488 W.Y., W-B.S. and Z.W. conceived and designed the experiments. W.Y., M.L., H.Y. and Y.H.
489 performed the experiments. W.Y., J.Z., G.L., W-B.S. and Z.W analyzed the data. W.Y., H.Y., W-
490 B.S. and Z.W. wrote the paper.
491

492 **Acknowledgments**

493 This work was supported by the NSFC grants (#31601599) and Science and Technology
494 Innovation Special Fund of FAFU(#CXZX2017138).

495
496

497 **References**

498

499 **Agne, B., Meindl, N. M., Niederhoff, K., Einwachter, H., Rehling, P., Sickmann, A., Meyer,**
500 **H. E., Girzalsky, W. and Kunau, W. H.** (2003) Pex8p: An intraperioxisomal organizer
501 of the peroxisomal import machinery. *Mol Cell,* **11,** 635-646.
502 **Alberts, B., Johnson, A., Lewis, J., Raff, M., Roberts, K. and Walter, P.** (2002) Peroxisomes.
503 In: *Mol Biol Cell.* New York: Garland Science.
504 **Bauer, S. and Morris, M. T.** (2017) Glycosome biogenesis in trypanosomes and the *de novo*
505 dilemma. *Plos Neglect Trop D,* **11,** e0005333.
506 **Bellu, A. R., Komori, M., van der Klei, I. J., Kiel, J. A. and Veenhuis, M.** (2001) Peroxisome
507 biogenesis and selective degradation converge at Pex14p. *J Biol Chem,* **276,** 44570-44574.
508 **Boisson-Dernier, A., Frietsch, S., Kim, T. H., Dizon, M. B. and Schroeder, J. I.** (2008) The
509 peroxin loss-of-function mutation abstinence by mutual consent disrupts male-female
510 gametophyte recognition. *Curr Biol,* **18,** 63-68.
511 **Bojja, R. S., Cerny, R. L., Proctor, R. H. and Du, L.** (2004) Determining the biosynthetic
512 sequence in the early steps of the fumonisin pathway by use of three gene-disruption
513 mutants of *Fusarium verticillioides*. *J Agric Food Chem,* **52,** 2855-2860.
514 **Brady, R. N., Di Mari, S. J. and Snell, E. E.** (1969) Biosynthesis of sphingolipid bases. 3.
515 Isolation and characterization of ketonic intermediates in the synthesis of sphingosine and
516 dihydrosphingosine by cell-free extracts of *Hansenula ciferri*. *J Biol Chem,* **244,** 491-496.
517 **Brown, D. W., Butchko, R. A., Busman, M. and Proctor, R. H.** (2007) The *Fusarium*
518 *verticillioides FUM* gene cluster encodes a Zn(II)2Cys6 protein that affects *FUM* gene
519 expression and fumonisin production. *Eukaryotic Cell,* **6,** 1210-1218.
520 **Chan, A., Schummer, A., Fischer, S., Schroter, T., Cruz-Zaragoza, L. D., Bender, J., Drepper,**
521 **F., Oeljeklaus, S., Kunau, W. H., Girzalsky, W., Warscheid, B. and Erdmann, R.**
522 (2016) Pex17p-dependent assembly of Pex14p/Dyn2p-subcomplexes of the peroxisomal
523 protein import machinery. *Eur J Cell Biol,* **95,** 585-597.
524 **Chen, Y., Zheng, S., Ju, Z., Zhang, C., Tang, G., Wang, J., Wen, Z., Chen, W. and Ma, Z.**
525 (2018) Contribution of peroxisomal docking machinery to mycotoxin biosynthesis,
526 pathogenicity and pexophagy in the plant pathogenic fungus *Fusarium graminearum*.
527 *Environmental Microbiology,* **20,** 3224-3245.
528 **Cho, D. H., Kim, Y. S., Jo, D. S., Choe, S. K. and Jo, E. K.** (2018) Pexophagy: Molecular
529 Mechanisms and Implications for Health and Diseases. *Mol Cells,* **41,** 55-64.
530 **Cooper, G. M.** (2000) Bioenergetics and Metabolism - Mitochondria, Chloroplasts, and
531 Peroxisomes. In: *The Cell: A Molecular Approach.* Sunderland, MA: Sinauer Associates.
532 **Deckers, M., Emmrich, K., Girzalsky, W., Awa, W. L., Kunau, W. H. and Erdmann, R.** (2010)
533 Targeting of Pex8p to the peroxisomal importomer. *Eur J Cell Biol,* **89,** 924-931.
534 **Deng, Y., Qu, Z. and Naqvi, N. I.** (2013) The role of snx41-based pexophagy in *Magnaporthe*
535 development. *PLoS One,* **8,** e79128.
536 **Desjardins, A. E. and Proctor, R. H.** (2007) Molecular biology of Fusarium mycotoxins. *Int J*
537 *Food Microbiol,* **119,** 47-50.
538 **Dixit, E., Boulant, S., Zhang, Y., Lee, A. S., Odendall, C., Shum, B., Hacohen, N., Chen, Z.**
539 **J., Whelan, S. P., Fransen, M., Nibert, M. L., Superti-Furga, G. and Kagan, J. C.**
540 (2010) Peroxisomes are signaling platforms for antiviral innate immunity. *Cell,* **141,** 668-
541 681.

542 **Einerhand, A. W. C., Kos, W., Smart, W. C., Kal, A. J., Tabak, H. F. and Cooper, T. G.** (1995)
543 The upstream region of the Fox3 gene encoding peroxisomal 3-oxoacyl-coenzyme-A
544 thiolase in *Saccharomyces cerevisiae* contains Abf1-binding and replication protein-A-
545 binding sites that participate in its regulation by glucose repression. *Mol Cell Biol,* **15,**
546 3405-3414.
547 **Erdmann, R. and Blobel, G.** (1996) Identification of Pex13p a peroxisomal membrane receptor
548 for the PTS1 recognition factor. *J Cell Biol,* **135,** 111-121.
549 **Farre, J. C., Manjithaya, R., Mathewson, R. D. and Subramani, S.** (2008) PpAtg30 tags
550 peroxisomes for turnover by selective autophagy. *Dev Cell,* **14,** 365-376.
551 **Fujihara, N., Sakaguchi, A., Tanaka, S., Fujii, S., Tsuji, G., Shiraishi, T., O'Connell, R. and**
552 **Kubo, Y.** (2010) Peroxisome biogenesis factor *PEX13* is required for appressorium-
553 mediated plant infection by the anthracnose fungus *Colletotrichum orbiculare*. *Mol Plant*
554 *Microbe Interact,* **23,** 436-445.
555 **Gabaldon, T.** (2010) Peroxisome diversity and evolution. *Philos Trans R Soc Lond B Biol Sci,*
556 **365,** 765-773.
557 **Girzalsky, W., Saffian, D. and Erdmann, R.** (2010) Peroxisomal protein translocation. *BBA -*
558 *Mol Cell Res,* **1803,** 724-731.
559 **Goh, J., Jeon, J., Kim, K. S., Park, J., Park, S. Y. and Lee, Y. H.** (2011) The *PEX7*-mediated
560 peroxisomal import system is required for fungal development and pathogenicity in
561 *Magnaporthe oryzae*. *PLoS One,* **6,** e28220.
562 **Grant, P., Ahlemeyer, B., Karnati, S., Berg, T., Stelzig, I., Nenicu, A., Kuchelmeister, K.,**
563 **Crane, D. I. and Baumgart-Vogt, E.** (2013) The biogenesis protein PEX14 is an optimal
564 marker for the identification and localization of peroxisomes in different cell types, tissues,
565 and species in morphological studies. *Histochem Cell Biol,* **140,** 423-442.
566 **Grunau, S., Schliebs, W., Linnepe, R., Neufeld, C., Cizmowski, C., Reinartz, B., Meyer, H.**
567 **E., Warscheid, B., Girzalsky, W. and Erdmann, R.** (2009) Peroxisomal targeting of
568 PTS2 pre-import complexes in the yeast *Saccharomyces cerevisiae*. *Traffic,* **10,** 451-460.
569 **Heiland, I. and Erdmann, R.** (2005) Biogenesis of peroxisomes - Topogenesis of the peroxisomal
570 membrane and matrix proteins. *Febs J,* **272,** 2362-2372.
571 **Herr, A. and Fischer, R.** (2014) Improvement of *Aspergillus nidulans* penicillin production by
572 targeting AcvA to peroxisomes. *Metab Eng,* **25,** 131-139.
573 **Hilton, A., Zhang, H. M., Yu, W. Y. and Shim, W. B.** (2017) Identification and characterization
574 of pathogenic and endophytic fungal species associated with Pokkah Boeng disease of
575 sugarcane. *Plant Pathology J,* **33,** 238-248.
576 **Hu, J., Baker, A., Bartel, B., Linka, N., Mullen, R. T., Reumann, S. and Zolman, B. K.** (2012)
577 Plant peroxisomes: biogenesis and function. *Plant Cell,* **24,** 2279-2303.
578 **Imazaki, A., Tanaka, A., Harimoto, Y., Yamamoto, M., Akimitsu, K., Park, P. and Tsuge, T.**
579 (2010) Contribution of peroxisomes to secondary metabolism and pathogenicity in the
580 fungal plant pathogen *Alternaria alternata*. *Eukaryot Cell,* **9,** 682-694.
581 **Jedd, G. and Chua, N. H.** (2000) A new self-assembled peroxisomal vesicle required for efficient
582 resealing of the plasma membrane. *Nat Cell Biol,* **2,** 226-231.
583 **Kimura, A., Takano, Y., Furusawa, I. and Okuno, T.** (2001) Peroxisomal metabolic function
584 is required for appressorium-mediated plant infection by *Colletotrichum lagenarium*. *Plant*
585 *Cell,* **13,** 1945-1957.
586 **Lazarow, P. B.** (2003) Peroxisome biogenesis: advances and conundrums. *Curr Opin Cell Biol,*
587 **15,** 489-497.

588 **Lee, M. Y., Sumpter, R., Jr., Zou, Z., Sirasanagandla, S., Wei, Y., Mishra, P., Rosewich, H.,**
589 **Crane, D. I. and Levine, B.** (2017) Peroxisomal protein PEX13 functions in selective
590 autophagy. *EMBO Rep,* **18,** 48-60.
591 **Leslie, J. F. and Summerell, B. A.** (2006) *The Fusarium Laboratory Manual*. Ames, Iowa:
592 Blackwell Publishing.
593 **Li, L., Wang, J., Chen, H., Chai, R., Zhang, Z., Mao, X., Qiu, H., Jiang, H., Wang, Y. and**
594 **Sun, G.** (2017) Pex14/17, a filamentous fungus-specific peroxin, is required for the import
595 of peroxisomal matrix proteins and full virulence of *Magnaporthe oryzae*. *Mol Plant*
596 *Pathol,* **18,** 1238-1252.
597 **Lin, Z. Y., Xu, S. Q., Que, Y. X., Wang, J. H., Comstock, J. C., Wei, J. J., McCord, P. H.,**
598 **Chen, B. S., Chen, R. K. and Zhang, M. Q.** (2014) Species-specific detection and
599 identification of *Fusarium* species complex, the causal agent of sugarcane Pokkah Boeng
600 in China. *PLoS One,* **9**.
601 **Ma, C., Schumann, U., Rayapuram, N. and Subramani, S.** (2009) The peroxisomal matrix
602 import of Pex8p requires only PTS receptors and Pex14p. *Mol Biol Cell,* **20,** 3680-3689.
603 **Maggio-Hall, L. A., Wilson, R. A. and Keller, N. P.** (2005) Fundamental contribution of beta-
604 oxidation to polyketide mycotoxin production in planta. *Mol Plant Microbe Interact,* **18,**
605 783-793.
606 **Managadze, D., Wurtz, C., Sichting, M., Niehaus, G., Veenhuis, M. and Rottensteiner, H.**
607 (2007) The peroxin PEX14 of *Neurospora crassa* is essential for the biogenesis of both
608 glyoxysomes and Woronin bodies. *Traffic,* **8,** 687-701.
609 **Managadze, D., Wurtz, C., Wiese, S., Schneider, M., Girzalsky, W., Meyer, H. E., Erdmann,**
610 **R., Warscheid, B. and Rottensteiner, H.** (2010) Identification of PEX33, a novel
611 component of the peroxisomal docking complex in the filamentous fungus *Neurospora*
612 *crassa*. *Eur J Cell Biol,* **89,** 955-964.
613 **Marin, S., Ramos, A. J., Cano-Sancho, G. and Sanchis, V.** (2013) Mycotoxins: Occurrence,
614 toxicology, and exposure assessment. *Food Chem Toxicol,* **60,** 218-237.
615 **Martin, J. F., Ullan, R. V. and Garcia-Estrada, C.** (2012) Role of peroxisomes in the
616 biosynthesis and secretion of beta-lactams and other secondary metabolites. *J Ind*
617 *Microbiol Biotechnol,* **39,** 367-382.
618 **Meinecke, M., Cizmowski, C., Schliebs, W., Kruger, V., Beck, S., Wagner, R. and Erdmann,**
619 **R.** (2010) The peroxisomal importomer constitutes a large and highly dynamic pore. *Nat*
620 *Cell Biol,* **12,** 273-277.
621 **Min, K., Son, H., Lee, J., Choi, G. J., Kim, J. C. and Lee, Y. W.** (2012) Peroxisome function is
622 required for virulence and survival of *Fusarium graminearum*. *Mol Plant Microbe Interact,*
623 **25,** 1617-1627.
624 **Montilla-Martinez, M., Beck, S., Klumper, J., Meinecke, M., Schliebs, W., Wagner, R. and**
625 **Erdmann, R.** (2015) Distinct pores for peroxisomal import of PTS1 and PTS2 proteins.
626 *Cell Rep,* **13,** 2126-2134.
627 **Nguyen, L. N., Bormann, J., Le, G. T., Starkel, C., Olsson, S., Nosanchuk, J. D., Giese, H.**
628 **and Schafer, W.** (2011) Autophagy-related lipase FgATG15 of *Fusarium graminearum*
629 is important for lipid turnover and plant infection. *Fungal Genet Biol,* **48,** 217-224.
630 **Nuttall, J. M., Motley, A. and Hettema, E. H.** (2011) Peroxisome biogenesis: recent advances.
631 *Curr Opin Cell Biol,* **23,** 421-426.

632 **Opalinski, L., Kiel, J. A., Homan, T. G., Veenhuis, M. and van der Klei, I. J.** (2010)
633 *Penicillium chrysogenum* Pex14/17p--a novel component of the peroxisomal membrane
634 that is important for penicillin production. *Febs J,* **277,** 3203-3218.
635 **Opalinski, L., Kiel, J. A. K. W., Williams, C., Veenhuis, M. and van der Klei, I. J.** (2011)
636 Membrane curvature during peroxisome fission requires Pex11. *Embo J,* **30,** 5-16.
637 **Peraza-Reyes, L., Arnaise, S., Zickler, D., Coppin, E., Debuchy, R. and Berteaux-Lecellier,**
638 **V.** (2011) The importomer peroxins are differentially required for peroxisome assembly
639 and meiotic development in *Podospora anserina*: insights into a new peroxisome import
640 pathway. *Mol Microbiol,* **82,** 365-377.
641 **Pieuchot, L. and Jedd, G.** (2012) Peroxisome assembly and functional diversity in eukaryotic
642 microorganisms. *Annual Review of Microbiology,* **66,** 237-263.
643 **Pires, J. R., Hong, X., Brockmann, C., Volkmer-Engert, R., Schneider-Mergener, J.,**
644 **Oschkinat, H. and Erdmann, R.** (2003) The ScPex13p SH3 domain exposes two distinct
645 binding sites for Pex5p and Pex14p. *J Mol Biol,* **326,** 1427-1435.
646 **Platta, H. W., Hagen, S. and Erdmann, R.** (2013) The exportomer: the peroxisomal receptor
647 export machinery. *Cell Mol Life Sci,* **70,** 1393-1411.
648 **Ramos-Pamplona, M. and Naqvi, N. I.** (2006) Host invasion during rice-blast disease requires
649 carnitine-dependent transport of peroxisomal acetyl-CoA. *Mol Microbiol,* **61,** 61-75.
650 **Rayapuram, N. and Subramani, S.** (2006) The importomer - A peroxisomal membrane complex
651 involved in protein translocation into the peroxisome matrix. *BBA - Mol Cell Res,* **1763,**
652 1613-1619.
653 **Rehling, P., Skaletz-Rorowski, A., Girzalsky, W., Voorn-Brouwer, T., Franse, M. M., Distel,**
654 **B., Veenhuis, M., Kunau, W. H. and Erdmann, R.** (2000) Pex8p, an intraperoxisomal
655 peroxin of *Saccharomyces cerevisiae* required for protein transport into peroxisomes binds
656 the PTS1 receptor Pex5p. *Journal of Biological Chemistry,* **275,** 3593-3602.
657 **Reverberi, M., Punelli, M., Smith, C. A., Zjalic, S., Scarpari, M., Scala, V., Cardinali, G.,**
658 **Aspite, N., Pinzari, F., Payne, G. A., Fabbri, A. A. and Fanelli, C.** (2012) How
659 peroxisomes affect aflatoxin biosynthesis in *Aspergillus flavus*. *PLoS One,* **7,** e48097.
660 **Rocha, L. O., Barroso, V. M., Andrade, L. J., Pereira, G. H., Ferreira-Castro, F. L., Duarte,**
661 **A. P., Michelotto, M. D. and Correa, B.** (2015) *FUM* gene expression profile and
662 fumonisin production by *Fusarium verticillioides* inoculated in Bt and non-Bt maize. *Front*
663 *Microbiol,* **6,** 1503.
664 **Saikia, S. and Scott, B.** (2009) Functional analysis and subcellular localization of two
665 geranylgeranyl diphosphate synthases from *Penicillium paxilli*. *Mol Genet Genomics,* **282,**
666 257-271.
667 **Schell-Steven, A., Stein, K., Amoros, M., Landgraf, C., Volkmer-Engert, R., Rottensteiner,**
668 **H. and Erdmann, R.** (2005) Identification of a novel, intraperoxisomal pex14-binding site
669 in pex13: association of pex13 with the docking complex is essential for peroxisomal
670 matrix protein import. *Mol Cell Biol,* **25,** 3007-3018.
671 **Soundararajan, S., Jedd, G., Li, X., Ramos-Pamplona, M., Chua, N. H. and Naqvi, N. I.** (2004)
672 Woronin body function in *Magnaporthe grisea* is essential for efficient pathogenesis and
673 for survival during nitrogen starvation stress. *Plant Cell,* **16,** 1564-1574.
674 **Suaste-Olmos, F., Zirion-Martinez, C., Takano-Rojas, H. and Peraza-Reyes, L.** (2018)
675 Meiotic development initiation in the fungus *Podospora anserina* requires the peroxisome
676 receptor export machinery. *Biochim et Biophys Acta - Mol Cell Res,* **1865,** 572-586.

677 **Thoms, S., Gronborg, S. and Gartner, J.** (2009) Organelle interplay in peroxisomal disorders.
678 *Trends Mol Med,* **15,** 293-302.
679 **Verplaetse, E., Gualdron-Lopez, M., Chevalier, N. and Michels, P. A. M.** (2012) Studies on
680 the organization of the docking complex involved in matrix protein import into glycosomes
681 of *Trypanosoma brucei*. *Biochem Bioph Res Co,* **424,** 781-785.
682 **Wang, J., Zhang, Z., Wang, Y., Li, L., Chai, R., Mao, X., Jiang, H., Qiu, H., Du, X., Lin, F.**
683 **and Sun, G.** (2013) PTS1 peroxisomal import pathway plays shared and distinct roles to
684 PTS2 pathway in development and pathogenicity of *Magnaporthe oryzae*. *PLoS One,* **8,**
685 e55554.
686 **Wang, Z. Y., Soanes, D. M., Kershaw, M. J. and Talbot, N. J.** (2007) Functional analysis of
687 lipid metabolism in *Magnaporthe grisea* reveals a requirement for peroxisomal fatty acid
688 beta-oxidation during appressorium-mediated plant infection. *Mol Plant Microbe Interact,*
689 **20,** 475-491.
690 **Waterham, H. R., Titorenko, V. I., Haima, P., Cregg, J. M., Harder, W. and Veenhuis, M.**
691 (1994) The *Hansenula polymorpha* Per1 gene is essential for peroxisome biogenesis and
692 encodes a peroxisomal matrix protein with both carboxy-terminal and amino-terminal
693 targeting signals. *Journal of Cell Biology,* **127,** 737-749.
694 **Woloshuk, C. P. and Shim, W. B.** (2013) Aflatoxins, fumonisins, and trichothecenes: a
695 convergence of knowledge. *Fems Microbiol Rev,* **37,** 94-109.
696 **Wu, F., Groopman, J. D. and Pestka, J. J.** (2014) Public Health Impacts of Foodborne
697 Mycotoxins. *Annual Review of Food Science and Technology,* **5,** 351-372.
698 **Yan, H. and Shim, W. B.** (2020) Characterization of non-canonical G beta-like protein FvGbb2
699 and its relationship with heterotrimeric G proteins in *Fusarium verticillioides*. *Environ*
700 *Microbiol,* **22,** 615-628.
701 **You, J., Hou, S., Malik-Soni, N., Xu, Z., Kumar, A., Rachubinski, R. A., Frappier, L. and**
702 **Hobman, T. C.** (2015) Flavivirus infection impairs peroxisome biogenesis and early
703 antiviral signaling. *J Virol,* **89,** 12349-12361.
704 **Zhang, C. K., Wang, J. Q., Tao, H., Dang, X., Wang, Y., Chen, M. P., Zhai, Z. Z., Yu, W. Y.,**
705 **Xu, L. P., Shim, W. B., Lu, G. D. and Wang, Z. H.** (2015) FvBck1, a component of cell
706 wall integrity MAP kinase pathway, is required for virulence and oxidative stress response
707 in sugarcane Pokkah Boeng pathogen. *Front Microbiol,* **6,** 1096.
708 **Zhang, F., Geng, L., Huang, L., Deng, J., Fasoyin, O. E., Yao, G. and Wang, S.** (2018a)
709 Contribution of peroxisomal protein importer AflPex5 to development and pathogenesis in
710 the fungus *Aspergillus flavus*. *Curr Genet,* **64,** 1335-1348.
711 **Zhang, H., Mukherjee, M., Kim, J. E., Yu, W. and Shim, W. B.** (2018b) Fsr1, a striatin
712 homologue, forms an endomembrane-associated complex that regulates virulence in the
713 maize pathogen *Fusarium verticillioides*. *Mol Plant Pathol,* **19,** 812-826.
714 **Zheng, W., Zhou, J., He, Y., Xie, Q., Chen, A., Zheng, H., Shi, L., Zhao, X., Zhang, C., Huang,**
715 **Q., Fang, K., Lu, G., Ebbole, D. J., Li, G., Naqvi, N. I. and Wang, Z.** (2015) Retromer
716 is essential for autophagy-dependent plant infection by the rice blast fungus. *PLoS Genet,*
717 **11,** e1005704.
718 **Zolman, B. K. and Bartel, B.** (2004) An Arabidopsis indole-3-butyric acid-response mutant
719 defective in PEROXIN6, an apparent ATPase implicated in peroxisomal function. *P Natl*
720 *Acad Sci USA,* **101,** 1786-1791.
721

722 **Figure legends**

723

724 **Fig. 1. FvPex8, FvPex13, FvPex14, and FvPex33 protein interaction analyses.**

725 (A) Localization of FvPex8-GFP, FvPex13-GFP, and FvPex33-GFP were studied in comparison
726 to FvPex14-mCherry, which was used as a peroxisomal marker, in the wild-type strain. Scale bar
727 = 10 μm. GFP-trap-based pull-down experiment showing the interaction *in vitro* between (B)
728 FvPex13 and FvPex14, (C) FvPex13 and FvPex8, (D) FvPex33 and FvPex14, and (E) FvPex8 and
729 FvPex14. The strains co-expressing the indicated proteins were immunoprecipitated with GFP trap
730 beads. The IP signal (FvPex13-GFP, FvPex8-GFP, or FvPex33-GFP) and the Co-IP signal
731 (FvPex14-mCherry or FvPex33-mCherry) were detected by immunoblots probed with antibodies
732 to GFP and mCherry, respectively.

733

734 **Fig. 2. Impact of FvPex8 on Pex gene transcription and carbon source utilization.**

735 (A) Expression changes of Peroxin genes were studied in each mutant using qPCR. Relative
736 transcript abundance was measured by qPCR and normalized to *F. verticillioides* β-tubulin gene.
737 Values are means ± SE of three replicates. (B) Vegetative growth and aerial mycelia production
738 in wild-type (WT) and mutant strains were monitored on minimal medium (MM) amended with
739 different carbon sources. Colony morphology was photographed after 5 days of incubation at 25°C.
740 (C) The growth inhibition rate was analyzed by comparing the growth of wild type with mutants
741 on MM agar with various carbon amendments. The mycelial growth inhibition rate (%) was
742 measured by [(the diameter of WT strain - the diameter of mutant strain)/(the diameter of WT
743 strain)]×100%). Bar indicates the standard deviation of three replicates.

744

745 **Fig. 3. Reactive oxygen species response in mutants**

746 (A) Fungal hyphae were grown for 2 days and stained with CM-H2DCFDA to measure cellular
747 ROS accumulation in wild-type strain Fv7600 and mutants. Accumulation of ROS in mycelia was
748 visualized with 6-chloromethyl-2',7'-dichlorodihydrofluorescein diacetate (CM-H2DCFDA)
749 staining. Scale bar = 10 μm. (B) ROS accumulation was quantified by Image J software. Error bars
750 represent the deviation from three replicates and the same letter indicates no differences at $P<0.05$
751 level. (C) Endogenous ROS scavenging capacity was tested by staining fungal strains grown on
752 CMII medium for 5 days with 3,3'-diaminobenzidine (DAB) for H_2O_2 detection and with Nitro
753 Blue Tetrazolium (NBT) for O^{2-} detection.

754

755 **Fig. 4. Disruption of peroxisomal functions promotes reactive oxygen species (ROS)**
756 **accumulation**.

757 (A) Mycelial growth of the wild type (WT) and mutants was monitored on CMII media
758 supplemented with sodium dodecyl sulfate (SDS), Calcofluor white (CFW), and H_2O_2 for 5 days.
759 Plates were photographed after 5 days of incubation at 25°C. (B) Mycelial growth inhibition rates
760 were calculated by [(the diameter of WT strain - the diameter of mutant strain)/(the diameter of
761 WT strain]×100%.

762

763 **Fig. 5. Role of peroxins in fumonisin B1 (FB1) production and *FUM* gene expression**

764 (A) Surface sterilized B73 corn kernels were inoculated with wild type (WT) and mutant fungal
765 conidia and were incubated for 10 days before FB1 levels were quantified by ELISA Kit. *F.*
766 *verticillioides* biomass was quantified by measuring *F. verticillioides* β-tubulin (*TUB2*) DNA in
767 samples. FB1 level in samples was normalized by calculating FB1 (ppm)/ *TUB2* DNA (ng). (B)

768 To compare the expression levels of key *FUM* genes, RNA samples were prepared from the wild
769 type (WT) and ΔFvpex8 mutant on corn kernel for 10 days. The expression levels of *FUM1*, *FUM8*,
770 *FUM19* and *FUM21* were normalized to *TUB2* expression. The experiment was repeated three
771 times, and error bars represent the standard deviation from three replicates.
772
773 **Fig. 6. Role of DTM peroxins in maize stalk rot virulence.**
774 (A) Maize B73 stalks were inoculated with wild type (WT) and mutant fungal spore suspension
775 (10^6/ml) at the internodal region and incubated at room temperature for 7 days. Subsequently,
776 maize stalks were split longitudinally to visually inspect rot symptoms. (B) Image J software was
777 used to quantify the extent of the rot in each sample. Three independent biological repetitions were
778 performed and error bars represent the standard deviation from three replicates. Sterile water was
779 used as a negative control (Fig. S5).
780
781 **Fig.7. Fvpex13 plays an important role in mycelial peroxin localization.**
782 (A) GFP fused to C-terminal PTS1 sequence (PTS1-GFP) and N-terminal PTS2 sequence (GFP-
783 PTS2), localizations were studied in the wild type (WT) and ΔFvpex13 mutant. Pex14-mCherry
784 signal was used as the peroxisomal marker. Bars = 2 μm. (B) Localization of key DTM peroxins
785 Pex8, Pex7, Pex19, and Pex5 were studied in the wild type (WT) and ΔFvpex13 mutant. Pex14
786 was monitored in ΔFvpex14 and ΔFvpex13, while Pex33-GFP was monitored in ΔFvpex33 and
787 ΔFvpex13.
788
789 **Fig. 8. Proposed schematic model of F. ve*rticillioides* peroxisome docking/translocation**
790 **module (DTM).**

791 The proposed model is based on our protein-protein interaction experiments as well as other
792 published fungal models. Our study showed that these proteins are involved in the regulation of
793 peroxisomal docking complex assembly and matrix translocation and ultimately impact various
794 aspects of fungal development, secondary metabolism, and virulence. Notably, we determined that
795 FvPex8 plays an important role in *F. verticillioides* mycotoxin biosynthesis. While we noticed
796 distinct role each component plays, FvPex13 was the key components in regulating virulence,
797 likely in close association with FvPex14 and FvPex33.
798
799 **Supplementary information**
800
801 **Table S1. Putative *F. verticillioides* DTM components identified by Blastp analysis**
802
803 **Table S2. *F. verticillioides* strains used in this study**
804
805 **Table S3. PCR primers used in this study.**
806
807 **Figure S1. Sequence analysis of Docking peroxin homologs in *F. verticillioides***
808 (A) Schematic description of conserveds domain in peroxins FvPex13, FvPex14 and FvPex33. (B)
809 Phylogenetic relationship of FvPex33 and its homologs calculated with neighbor joining method
810 using the MEGA 6.0 program according to the alignment. (C) Possible transmembrane helices
811 predicted in FvPex8, FvPex13, FvPex14, and FvPex33 analyzed by TMPRED algorithm.
812
813 **Figure S2. Docking protein interaction by yeast two hybrid assays.**

814 Interactions between DTM peroxins were tested using the yeast two-hybrid assay. Yeast
815 transformants expressing plasmids harboring the indicated constructs were assayed for growth on
816 selective plates (SD/Leu/Trp/His/Ade), and for β-galactosidase (LacZ) activities. The pGBKT7-
817 53/pGADT7-T and pGBKT7-Lam/pGADT7-T was used as positive and negative control,
818 respectively.
819
820 **Figure S3. Vegetative growth, growth inhibition of mutants.**
821 (A) The colony morphology of DTM mutants and the wild-type strain on CMII agar media and
822 linoleic acid medium. (B) Mycelial growth inhibition rates were calculated by [(the diameter of
823 WT strain - the diameter of mutant strain)/(the diameter of WT strain)]x100%. (C) conidiation in
824 the wild type and DTM mutants on CMII agar.
825
826 **Figure S4. Reduction in lipid droplet degradation and carbon sources utilization**
827 (A) Wild-type (WT) and mutant strains were grown for 2 days in rich medium, then transferred
828 to 1% potassium acetate medium and stained with Nile red to observe the lipid droplet formation
829 of the hyphae after starvation at 0 h and 18 h time points. (B) Lipid droplet gross area was
830 measured in each sample at 0 h and 18 h time points. (C) Lipid droplet sizes were measured
831 measured in each sample at 0 h and 18 h time points. Bars denote standard deviations from three
832 repeated experiments. The same letter on the bars for each treatment represents no significant
833 difference at P = 0.05.
834
835 **Figure S5. Role of DTM peroxins in sugarcane stalk rot virulence.**

836 (A) Sugarcane stalks (cultivar Badila) were inoculated with fungal spore suspension (10^6/ml) at
837 the internodal region and incubated in room temperature for 7 days. Subsequently, stalks were split
838 longitudinally to visually inspect rot symptoms. (B) Image J software was used to quantify the
839 extent of the rot in each sample. Three independent biological repetitions were performed and error
840 bars represent the standard deviation from three replicates. (C) Sterile water was used as a negative
841 control on maize stalk.
842
843

Yu et al. Fig. 1

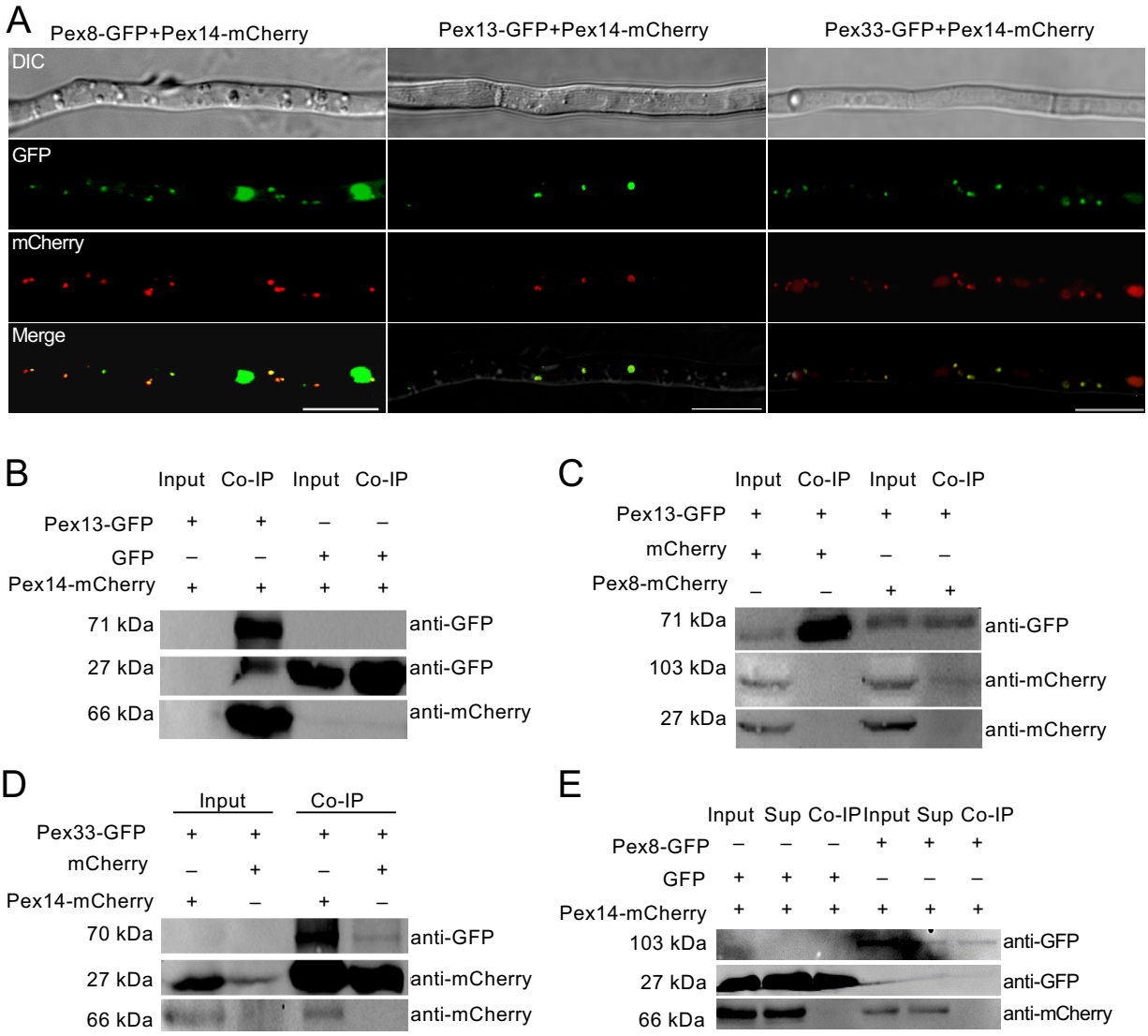
A
Pex8-GFP+Pex14-mCherry
Pex13-GFP+Pex14-mCherry
Pex33-GFP+Pex14-mCherry
DIC
GFP
mCherry
Merge
B
Input Co-IP Input Co-IP
Pex13-GFP + + – –
GFP – – + +
Pex14-mCherry + + + +
71 kDa anti-GFP
27 kDa anti-GFP
66 kDa anti-mCherry
C
Input Co-IP Input Co-IP
Pex13-GFP + + + +
mCherry + + – –
Pex8-mCherry – – + +
71 kDa anti-GFP
103 kDa anti-mCherry
27 kDa anti-mCherry
D
Input Co-IP
Pex33-GFP + + + +
mCherry – + – +
Pex14-mCherry + – + –
70 kDa anti-GFP
27 kDa anti-mCherry
66 kDa anti-mCherry
E
Input Sup Co-IP Input Sup Co-IP
Pex8-GFP – – – + + +
GFP + + + – – –
Pex14-mCherry + + + + + +
103 kDa anti-GFP
27 kDa anti-GFP
66 kDa anti-mCherry

Yu et al. Fig. 2

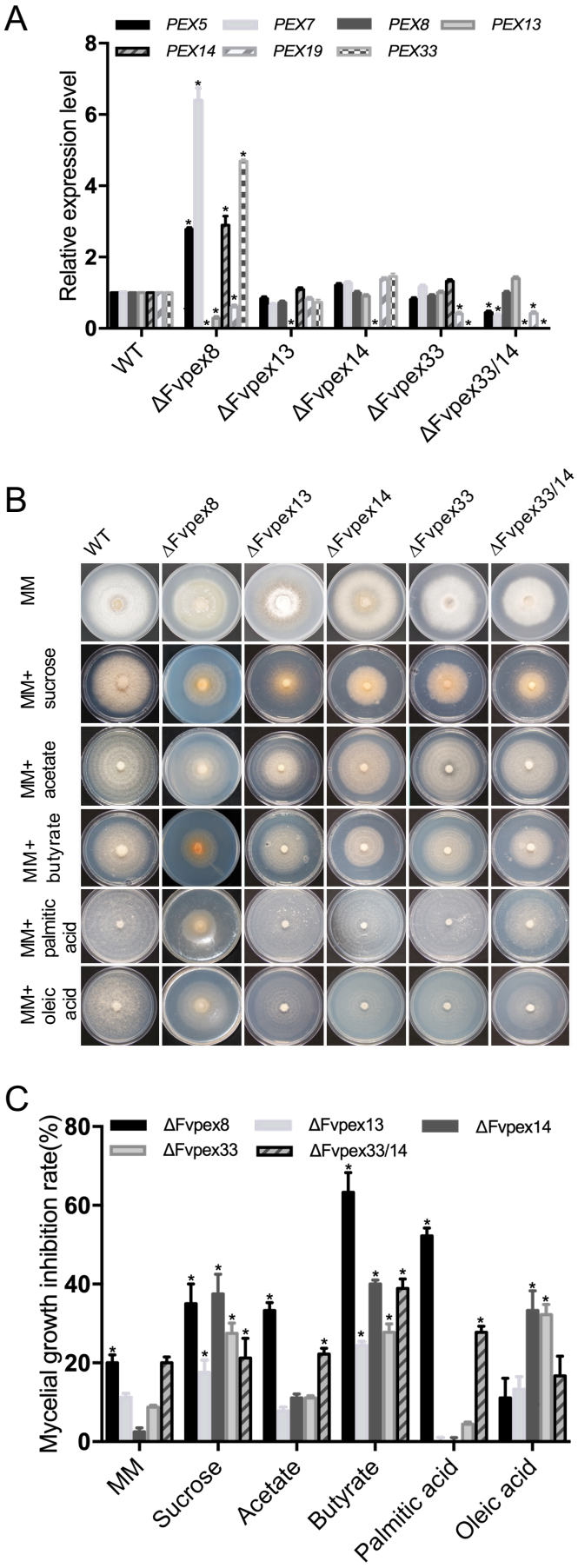
A
PEX5
PEX7
PEX8
PEX13
PEX14
PEX19
PEX33
Relative expression level
0
2
4
6
8
WT
ΔFvpex8
ΔFvpex13
ΔFvpex14
ΔFvpex33
ΔFvpex33/14
B
WT
ΔFvpex8
ΔFvpex13
ΔFvpex14
ΔFvpex33
ΔFvpex33/14
MM
MM+ sucrose
MM+ acetate
MM+ butyrate
MM+ palmitic acid
MM+ oleic acid
C
ΔFvpex8
ΔFvpex13
ΔFvpex14
ΔFvpex33
ΔFvpex33/14
Mycelial growth inhibition rate(%)
0
20
40
60
80
MM
Sucrose
Acetate
Butyrate
Palmitic acid
Oleic acid

Yu et al. Fig. 3

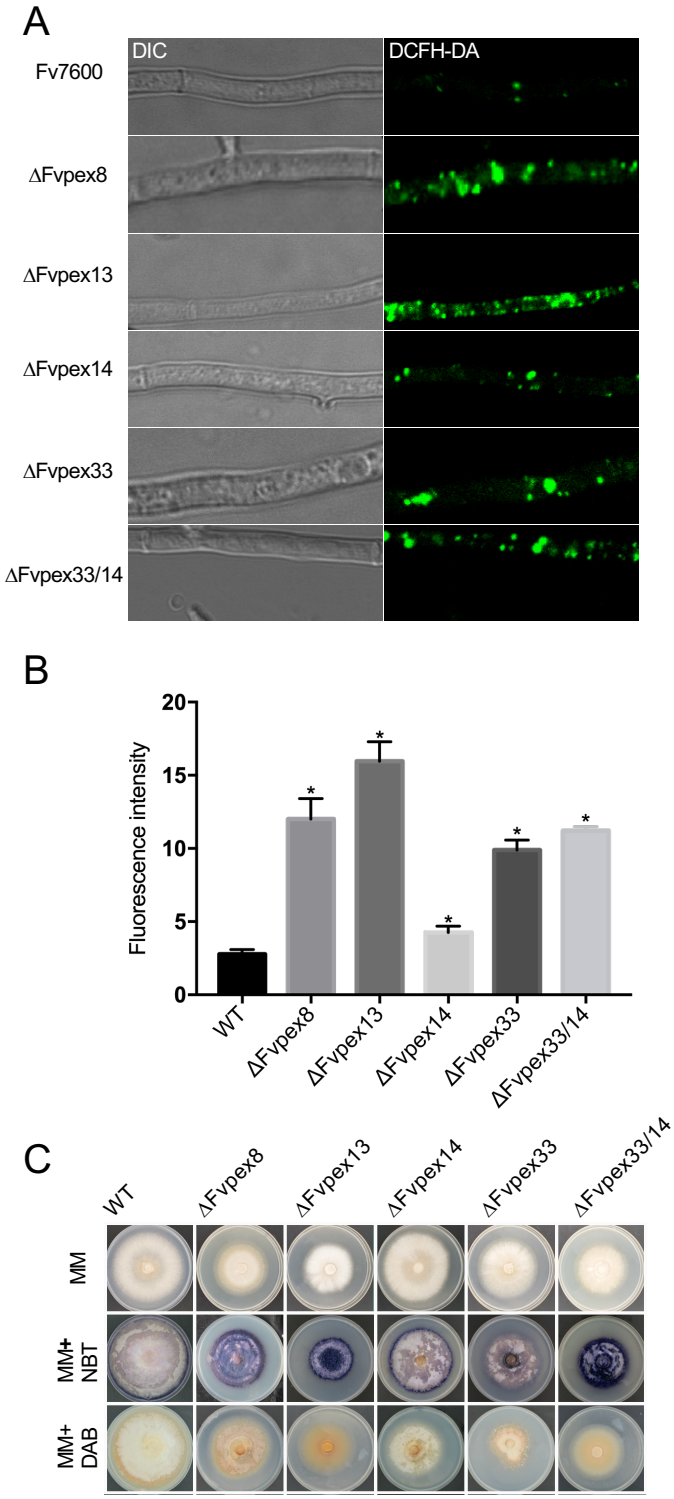
A
DIC
DCFH-DA
Fv7600
ΔFvpex8
ΔFvpex13
ΔFvpex14
ΔFvpex33
ΔFvpex33/14
B
Fluorescence intensity
20
15
10
5
0
WT
ΔFvpex8
ΔFvpex13
ΔFvpex14
ΔFvpex33
ΔFvpex33/14
C
WT
ΔFvpex8
ΔFvpex13
ΔFvpex14
ΔFvpex33
ΔFvpex33/14
MM
MM+ NBT
MM+ DAB

Yu et al. Fig. 4

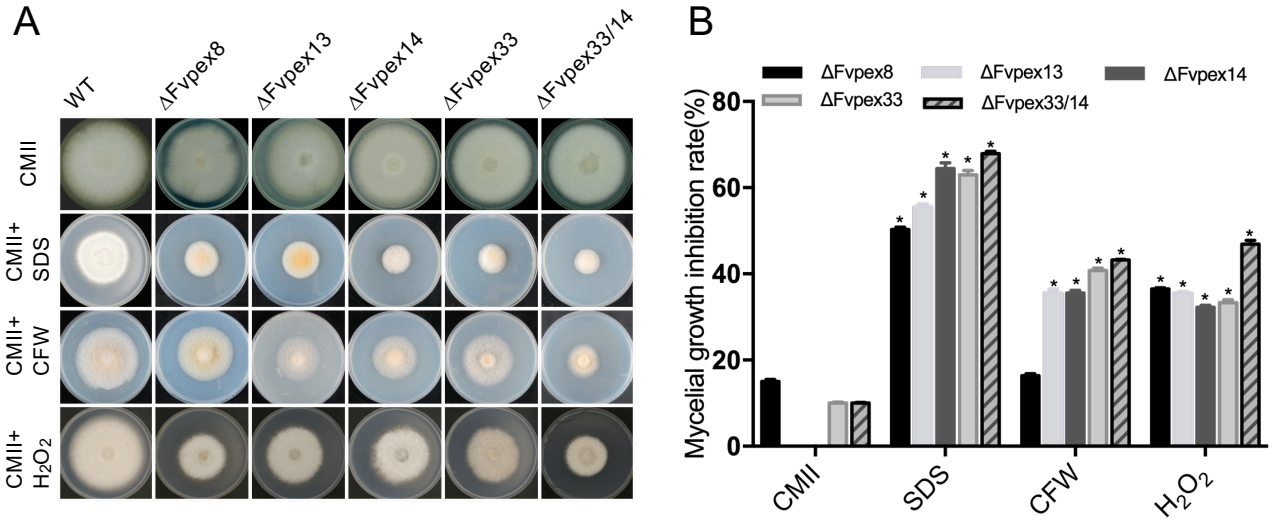
A
WT
ΔFvpex8
ΔFvpex13
ΔFvpex14
ΔFvpex33
ΔFvpex33/14
CMII
CMII+ SDS
CMII+ CFW
CMII+ H2O2
B
ΔFvpex8
ΔFvpex13
ΔFvpex14
ΔFvpex33
ΔFvpex33/14
Mycelial growth inhibition rate(%)
0
20
40
60
80
CMII
SDS
CFW
H2O2

Yu et al. Fig. 5

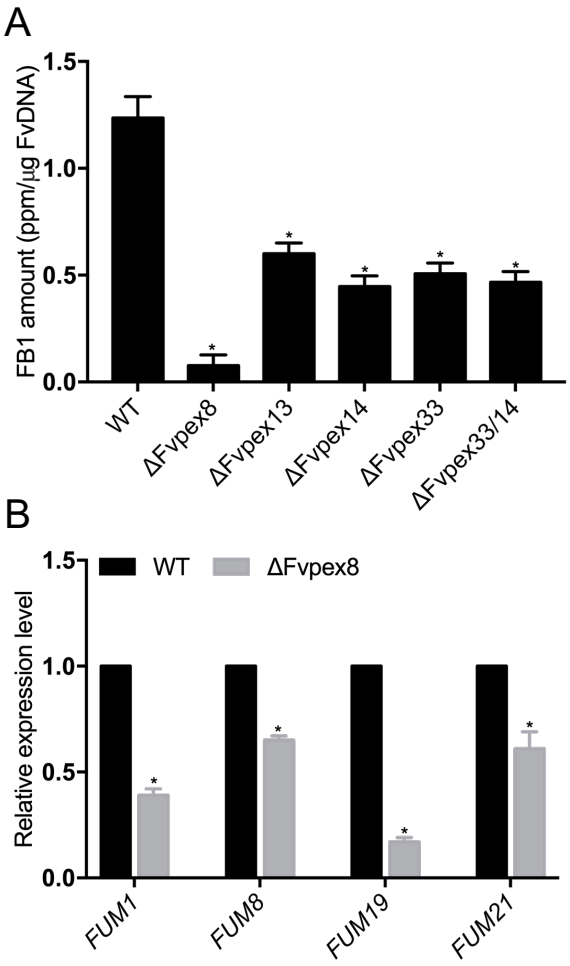
A
FB1 amount (ppm/μg FvDNA)
1.5
1.0
0.5
0.0
WT
ΔFvpex8
ΔFvpex13
ΔFvpex14
ΔFvpex33
ΔFvpex33/14
B
WT
ΔFvpex8
Relative expression level
1.5
1.0
0.5
0.0
FUM1
FUM8
FUM19
FUM21

Yu et al. Fig. 6

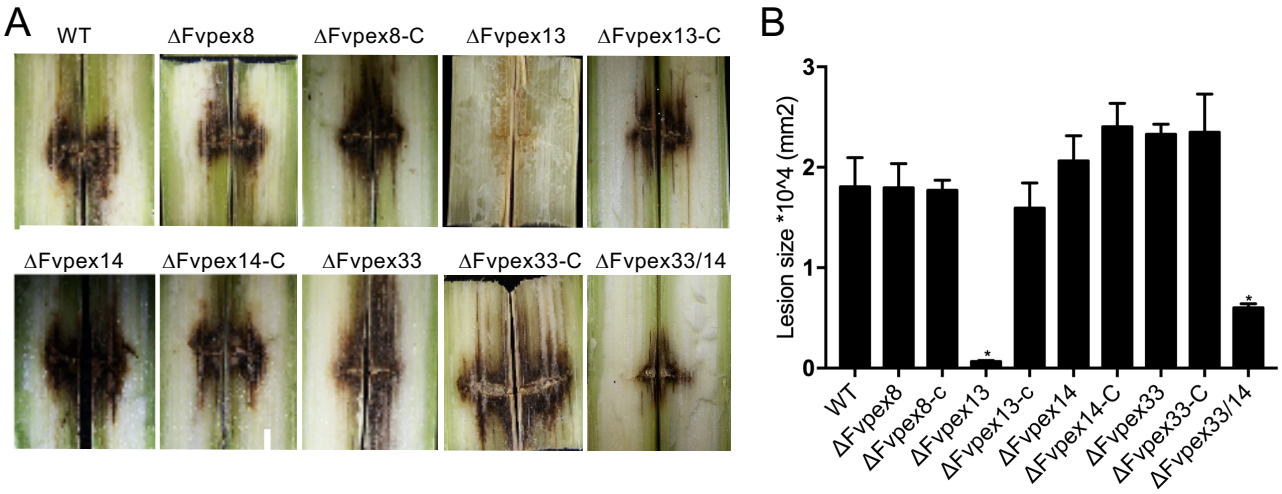
A
WT
ΔFvpex8
ΔFvpex8-C
ΔFvpex13
ΔFvpex13-C
ΔFvpex14
ΔFvpex14-C
ΔFvpex33
ΔFvpex33-C
ΔFvpex33/14
B
Lesion size *10^4 (mm2)
0
1
2
3
*
*
WT
ΔFvpex8
ΔFvpex8-c
ΔFvpex13
ΔFvpex13-c
ΔFvpex14
ΔFvpex14-C
ΔFvpex33
ΔFvpex33-C
ΔFvpex33/14

Yu et al. Fig. 7

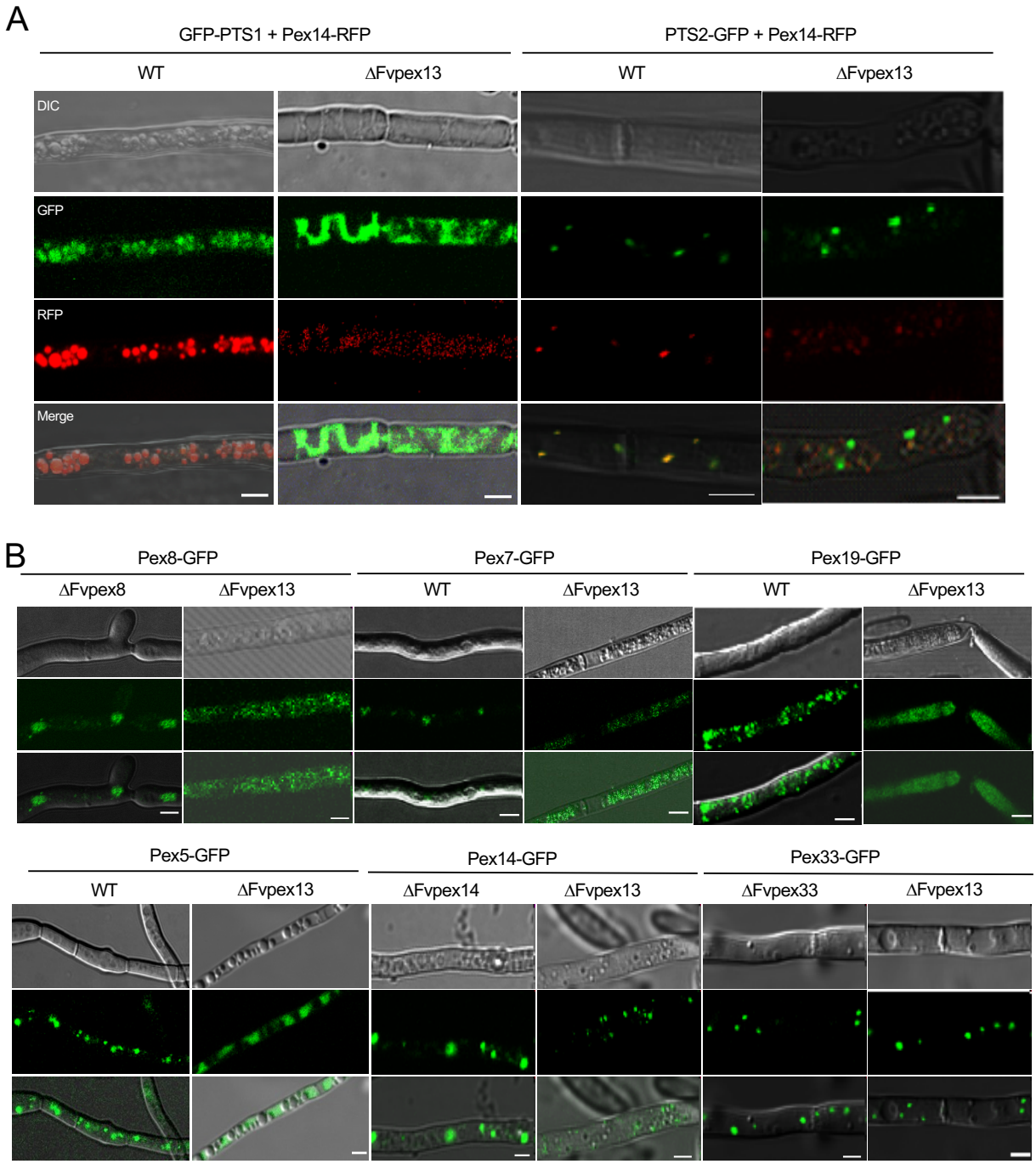
A
GFP-PTS1 + Pex14-RFP
PTS2-GFP + Pex14-RFP
WT
ΔFvpex13
WT
ΔFvpex13
DIC
GFP
RFP
Merge
B
Pex8-GFP
Pex7-GFP
Pex19-GFP
ΔFvpex8
ΔFvpex13
WT
ΔFvpex13
WT
ΔFvpex13
Pex5-GFP
Pex14-GFP
Pex33-GFP
WT
ΔFvpex13
ΔFvpex14
ΔFvpex13
ΔFvpex33
ΔFvpex13

Yu et al. Fig. 8

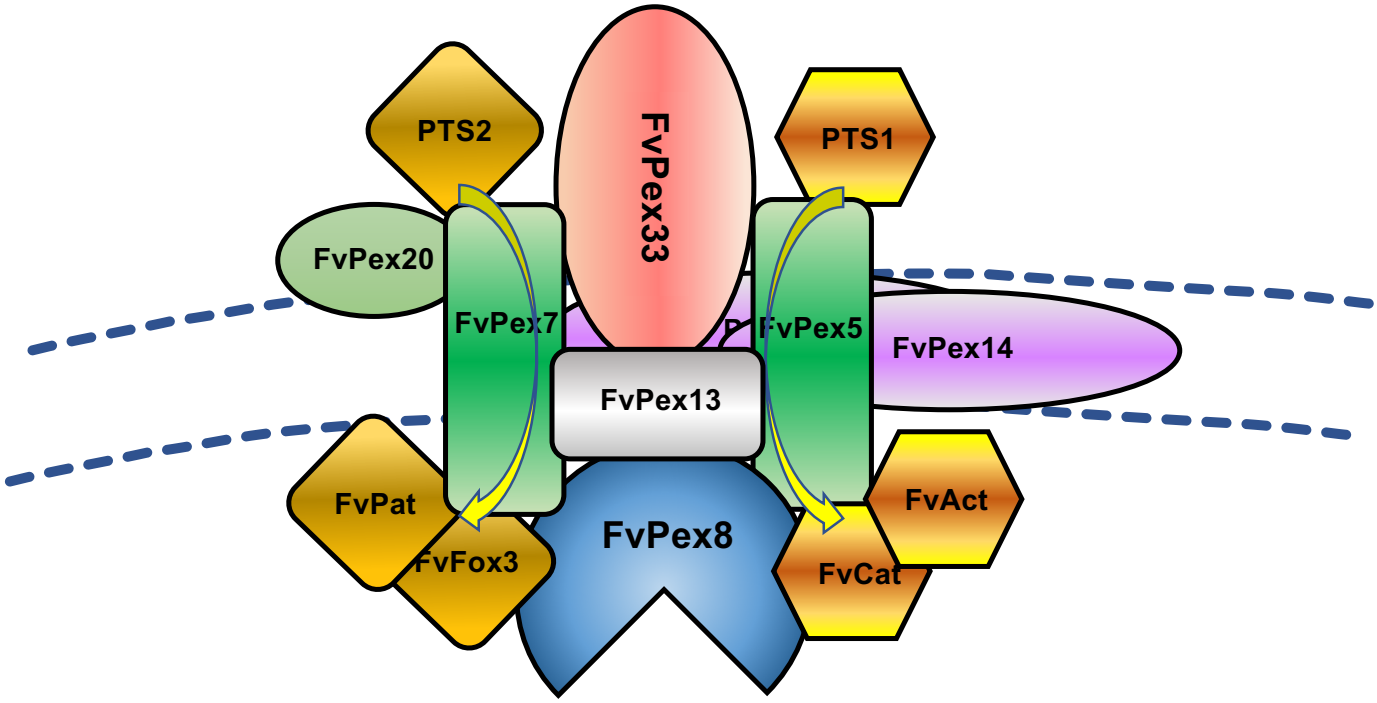
PTS2
FvPex33
PTS1
FvPex20
FvPex7
FvPex5
FvPex14
FvPex13
FvPat
FvFox3
FvPex8
FvCat
FvAct